



Treball Final de Grau

The $\text{NH}_3\text{-NH}_3$ intermolecular interaction: the $(\text{NH}_3)_{2-5}$ small ammonia clusters and liquid ammonia

Interacció intermolecular $\text{NH}_3\text{-NH}_3$: Petits clústers d'amoniac, $(\text{NH}_3)_{2-5}$, i amoníac líquid

Lluc Farrera Soler

January 2015

Aquesta obra esta subjecta a la llicència de:
Reconeixement–NoComercial–SenseObraDerivada



<http://creativecommons.org/licenses/by-nc-nd/3.0/es/>

*Millions saw the apple fall, Newton was the only
one who asked why.*

Bernard M. Baruch

I would like to show my gratitude to my advisor, Margarita Albertí, for all her dedication teaching me about molecular dynamics. Without the knowledge I learned from her, it would have been impossible to write this TFG.

REPORT

CONTENTS

1. SUMMARY	3
2. RESUM	5
3. INTRODUCTION	7
3.1. Molecular Dynamics Simulations	8
3.1.1. Microcanonical ensemble (NVE)	8
3.1.2. Isobaric-Isothermal ensemble (NpT)	9
3.2. The hydrogen bond in ammonia	10
3.2.1. Small ammonia clusters	11
3.2.2. Liquid ammonia	11
4. OBJECTIVES	16
5. THE $\text{NH}_3\text{-NH}_3$ INTERMOLECULAR INTERACTION	17
5.1. The Lennard Jones function	17
5.2. The Improved Lennard Jones function	18
5.3. The parameters of the Improved Lennard Jones function	19
5.4. The ILJ parameters for the $\text{NH}_3\text{-NH}_3$ interaction	21
6. THE SMALL $(\text{NH}_3)_{2-5}$ AGGREGATES	22
6.1. Estimation of the $(\text{NH}_3)_{2-5}$ binding energies	22
6.2. Quasi-linear and bent $\text{NH}\dots\text{N}$ contacts	24
7. LIQUID AMMONIA	31
7.1. Density and mean diffusion coefficients	31
7.2. Radial distribution functions and coordination number	32
8. CONCLUSIONS	37
9. REFERENCES AND NOTES	39
10. ACRONYMS	41
APPENDICES	43
Appendix 1: DL_POLY_2 files	

1. SUMMARY

Molecular Dynamics (MD) is a simulation technique that allows to analyse the interactions between atoms and molecules along the time, giving a visualization of the movement of the particles. For this simulation, an energy potential model describing the interaction needs to be implemented in MD programmes, giving us information directly comparable with experimental behaviour. MD simulations not only are useful for comparative purposes but also for predictive ones. Obviously, if we want to make predictions with a high guarantee of success, the model must be accurate. However, in order to reduce the simulation computational cost, the model has to be as simple as possible.

Ammonia is one of the most important compounds in nature because it contributes significantly to the nutritional needs of living organisms. In recent years, there have been a large number of accurate theoretical as well as experimental investigations on small ammonia clusters interactions, but not so many about liquid ammonia.

In order to represent big systems with lots of molecules (as required to simulate liquids), it is very important to have a function describing as good as possible the intermolecular interactions. In MD the previous interaction is often expressed as a sum of electrostatic and non electrostatic interaction contributions. The electrostatic one is usually defined by the Coulomb's law equation, whereas the non electrostatic one is often given by the Lennard Jones (LJ) potential. The LJ function, although it is quite good and widely used in MD simulations, it presents some problems. It is too repulsive at short distances, and too attractive at long distances. For this reason, the present TFG focuses on the study of ammonia using a modified LJ potential energy function (ILJ) to describe the non electrostatic contribution.

The ammonia study, according to the different properties of small clusters and liquid ammonia, has been divided in two parts. In the first one, the binding energy and equilibrium geometry of some small clusters, $(\text{NH}_3)_{2-5}$, have been calculated using the ILJ function and the results have been compared with other theoretical as well as experimental data. In the second part, once the reliability of the potential energy function has been proved, it has been applied to

investigate some characteristics of liquid ammonia. In particular, the evolution of the density values and of the diffusion coefficients with the temperature has been analysed. Moreover some structural properties of liquid ammonia have been compared with X-ray and neutron diffraction experimental data.

Keywords: force field, ammonia clusters, liquid ammonia, molecular dynamics.

2. RESUM

La dinàmica molecular (DM) és una tècnica de simulació que permet analitzar les interaccions entre àtoms i molècules al llarg del temps, donant una visualització del moviment de les partícules. Per això es necessita formular un model d'energia potencial utilitzable en programes de DM que ens permeti obtenir informació directament comparable amb el comportament experimental. Les simulacions de DM no només són útils amb finalitat comparativa, sinó també amb finalitat predictiva. Òbviament, per a que les prediccions tinguin una certa garantia d'èxit, el model ha de ser prou acurat. Per tal que les simulacions no siguin massa costoses des del punt de vista computacional, el model, tot i essent realista, haurà de ser el més senzill possible.

L'amoníac és una substància amb una gran importància degut a que contribueix significativament a les necessitats nutricionals dels organismes vius. Recentment s'han fet varis estudis, tant teòrics com experimentals, sobre les interaccions presents en els petits clústers d'amoníac, però pocs sobre l'amoníac líquid.

Per representar sistemes amb moltes molècules (l'estudi de líquids ho requereix) és molt important tenir una funció que descriu el millor possible les interaccions intermoleculars. En DM la interacció intermolecular s'acostuma a expressar com la suma d'interaccions electrostàtiques i no electrostàtiques. La interacció electrostàtica ve donada sovint per la Llei de Coulomb i la no electrostàtica normalment es defineix usant el potencial de Lennard Jones (LJ). Aquest últim, tot i ser força correcte i molt utilitzat en simulacions de DM, presenta alguns problemes: és massa repulsiu a distàncies curtes i massa atractiu a distàncies llargues. És per això que aquest treball se centre en l'estudi de l'amoníac descrivint la interacció no electrostàtica amb un potencial LJ modificat (I LJ).

L'estudi de l'amoníac, d'acord amb les diferents propietats dels petits clústers i de l'amoníac líquid, s'ha dut a terme en dues parts. En la primera, s'ha calculat l'energia d'enllaç i la geometria a l'equilibri d'alguns petits clústers d'amoníac $(\text{NH}_3)_{2-5}$ usant la funció d'energia potencial ILJ i els resultats s'han comparat amb altres dades teòriques i experimentals. A la

segona part, una vegada comprovat que la funció de potencial és prou acurada, s'ha aplicat a l'estudi de l'amoníac líquid. En concret, s'ha analitzat la variació dels valors de la densitat i dels coeficients de difusió amb la temperatura. A més, algunes propietats estructurals de l'amoníac líquid han estat comparades amb els resultats d'experiments de difracció de raigs X i de neutrons.

Paraules clau: camp de força, clústers d'amoníac, amoníac líquid, dinàmica molecular.

3. INTRODUCTION

Ammonia is a very important compound in nature because it contributes notably to the nutrition of living organisms by serving as a precursor to food and fertilizers. Moreover, it is very used for the synthesis of many pharmaceuticals and it is also present in many commercial cleaning products. Although in wide use, ammonia is both caustic and hazardous. Therefore, the theoretical investigation of ammonia interactions, which allow to understand the thermo-physical behaviour of ammonia and to plan experiments with a higher guarantee of success, is of fundamental importance. In recent years, there have been some accurate theoretical as well as experimental investigations on small ammonia clusters interactions. Most of these studies are performed only for selected geometries of the aggregates and, often, only structures close to the equilibrium are considered. However, in order to study large systems containing a large number of molecules, for instance liquid ammonia, it is very useful to represent the intermolecular interaction by means of analytical functions capable to represent attractive and repulsive zones of the potential energy surface. From this point of view, it would be interesting to have theoretical models giving information that helped to conduct experiments with a high guarantee of success.

Small aggregates are often studied using quantum methods (such as *ab initio*). However, due to the enormous computational cost, pure *ab initio* methods cannot be used to investigate large systems and the whole interaction is usually represented by analytical potential energy functions, the so-called force field (in the context of molecular modelling). From a computational point of view, it would be important to have a model represented by means of simple functions, containing only few parameters having a physical meaning and easily to be determined. Then, the quantum methods and experimental data can be used to corroborate if the suggested force field is appropriate for the system.

By modelling thermodynamic properties of small molecules like ammonia with force fields, it is commonly assumed that the intramolecular interactions are only of little importance. This is supported by the compact geometry of that molecule, exhibiting little configurational changes.

In this case, intramolecular interactions are not considered and the molecules are treated as rigid bodies. With respect to the thermodynamic properties of bulk fluid ammonia, it was shown that this simplification did not lead to serious errors.^{1,2}

In this study, we are interested in the construction of an intermolecular force field for ammonia that will be applied to investigate both some small ammonia clusters and liquid ammonia. These studies will be performed using Molecular Dynamics (MD) simulations. General details of the study are given in the present section. The main objectives are indicated in section 4. The construction of the force field is presented in section 5. The results of MD simulations for the small clusters and liquid ammonia are given in sections 6 and 7, respectively. Finally, the most important conclusions are given in section 8.

3.1 MOLECULAR DYNAMICS SIMULATIONS

MD simulation is a technique for computing the equilibrium and transport properties of a classical many-body system. The word classical means that the nuclear motion of the constituent particles obey the laws of classical mechanics. In MD simulations we select a model system consisting on N particles and we solve the classical equations of motion for this system until the properties of the system no longer change with time (equilibration of the system). After equilibration we perform the actual measurement of the properties. In order to measure an observable quantity in a MD simulation we must express this observable as a function of the positions and momenta of the system particles. There are different types of observables that can be measured in MD: thermodynamic properties of the system (temperature, pressure, etc.) and the functions that characterize the local structure of a fluid such as the radial distribution functions.

In MD simulations, different ensembles of particles can be considered. The choice depends on how a given property is calculated. In the present study, the small clusters are studied using the microcanonical ensemble (NVE), for which the number of particles (N), volume (V) and total energy (E), are conserved. On the contrary, liquid ammonia is investigated using an isobaric-isothermal ensemble (NpT), which allows a control of the pressure and of the temperature.

3.1.1 Microcanonical ensemble (NVE)

In the microcanonical ensemble (NVE), the system is isolated from changes in moles (N), volume (V) and total energy (E). It corresponds to an adiabatic process with no heat exchange.

A microcanonical molecular dynamics trajectory may be seen as an exchange of potential and kinetic energy, with total energy being conserved.

Constant-energy simulations are not recommended for equilibration because, without the energy flow facilitated by the temperature control methods, the desired temperature cannot be achieved. However, during the data collection phase, if one is interested in exploring the constant-energy surface of the conformational space, or, for other reasons do not want the perturbation introduced by temperature- and pressure- bath coupling, this is an useful ensemble.

It is the statistical ensemble used to represent the possible states of a mechanical system that has an exactly specified total energy. The system is assumed to be isolated in the sense that the system cannot exchange energy or particles with its environment, so that the energy of the system remains exactly known as time goes on.

In order to simulate a given temperature, a thermostat of some sort, like the Nose-Hoover or the Berendsen thermostat, needs to be implemented.³ These thermostats constantly adjust the particles' velocities so that they stay near a certain temperature.

3.1.2 Isobaric-Isothermal Ensemble (NpT)

The isothermal-isobaric ensemble³ represents a system of N molecules which is in thermal and mechanical contact with a very large bath, and which therefore exchanges energy and volume with the bath at constant temperature (T) and constant pressure (p) so that the energy (E) and the volume (V) of the system fluctuate. Such situation is realized by enclosing the system in a cylinder which is embedded in a very large bath, and which is sealed by a movable, frictionless and weightless piston P (see Figure 1).

In spite of the fact that the NVT ensemble allows to define the desired value of the density, the study of the systems at different temperatures is better represented by the NpT ensemble. This is one of the most frequently used ensembles, which is not surprising because it corresponds most closely to laboratory conditions (a flask open to ambient temperature and pressure). It is often convenient to use constant-NpT to simulate systems in the vicinity of a first-order phase transition, because at constant pressure the system is free (given enough time, of course) to transform completely into the state of lowest (Gibbs) free energy.

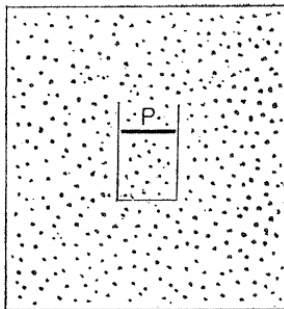


Figure 1. Isobaric-isothermal ensemble.⁴

3.2 THE HYDROGEN BOND IN AMMONIA

Ammonia, as one of the most important molecules in nature, is able to form hydrogen bonded networks. Moreover, among hydrogen-bonded dimers, $\text{NH}_3\text{-NH}_3$ is peculiar since it features a rather unusual hydrogen-bond. In particular, the issue of a quasilinear hydrogen bond versus a cyclic structure remained controversial up to 1990. Thanks to sophisticated experiments and extensive computations there is now consensus that the ammonia dimer is a fluxional molecular complex with an equilibrium structure characterized by a bent hydrogen bond.⁵ However, the potential energy surface is very flat and the cyclic structure was estimated to be only about 7 cm^{-1} higher in energy than the most stable ammonia dimer, which is consistent with the observation that the dimer is a very fluxional complex.⁵

In general, hydrogen-bonded dimers are inherently interesting, and their study provides insights into interactions that are important in a host of condensed phase and biological systems. However, despite the importance of ammonia in many fields of science and technology, less attention has been paid to the intermolecular interaction between ammonia molecules compared with water molecules. As a matter of fact, small ammonia clusters have been poorly investigated in comparison with small clusters of water and while a lot of structural information of liquid water can be found in the literature, only few studies exist for liquid ammonia. The previous observations suggest the importance of investigating the behavior of hydrogen bond in both the small gas phase ammonia clusters and liquid ammonia.

3.2.1. Small ammonia clusters

The dimer is the most investigated cluster of ammonia. Recent experiments using infrared excitation in combination with velocity-map ion imaging provide information on the dissociation energy of the $\text{NH}_3\text{-NH}_3$ dimer ($D_0 = 660 \pm 20 \text{ cm}^{-1}$).⁶ This value falls within the broad limits established by previous measurements. Scattering experiments place the lower bound at 520 cm^{-1} ⁷ and infrared dissociation measurements⁷ give an upper bound of 950 cm^{-1} .

Theoretical calculations, most commonly provide the well depth, D_e . Calculations of D_e at MP2/aug-cc-pVTZ level report a value of 1151 cm^{-1} ⁸, which decrease to a D_0 value of 661 cm^{-1} by including the zero-point energy contribution. Other authors, at the same level of calculation report a value of D_0 equal to 567 cm^{-1} ⁹. The estimation of zero point energy in a loosely bound complex as $\text{NH}_3\text{-NH}_3$ complex can be a difficult task. In quantum Monte Carlo simulations, Curoto and Mella¹⁰ determined that the zero point energy contribution was 42 % of the total binding energy, giving values of D_e and D_0 , equal to 1034 cm^{-1} and 603 cm^{-1} , respectively. Structures and binding energies of small ammonia clusters have been calculated using different properties of monomer ammonia.¹¹ As a matter of fact, geometries and binding energies for $(\text{NH}_3)_n$ ($n=2-5$) clusters were obtained using different models, which assume different charge distribution on NH_3 ¹² with dipole moments ranging from 1.46 D to 1.64 D. Most of these charge distributions correspond to a four-charge model. However, also an eight-point charge distribution (charges on the four atoms, on the three bonds and another one representing the lone pair), compatible with the dipole moment of 1.46 D is also considered (ABEEM ammonia-8P model).¹²

3.2.2. Liquid ammonia

As regarding liquid ammonia, structural details can be obtained from the N-N, N-H and H-H radial distribution functions (RDFs), which can be estimated from a theoretical point of view by analysing the dynamical properties of the system. X-ray¹³ and neutron diffraction techniques¹⁴ have been used to study the microscopic structure of liquid ammonia. In ref. 13 a complete set of neutron diffraction experiments with isotopic substitution is made at two different temperatures.

A RDF (or pair correlation function, $g(r)$) in a system of particles (atoms, molecules, colloids, etc.), describes how density varies as a function of the distance from a reference particle. It is a measure of the probability of finding a particle at a distance r away from a given reference particle. The general algorithm involves the determination of how many particles are within a distance of r and $r+\Delta r$ away from a particle, as schematized in Figure 2.

The construction of a radial distribution function is simple and it consist in the consideration of an atom of reference, drawing around it series of concentric spheres, set a small fixed distance (Δr) apart (see Figure 2).

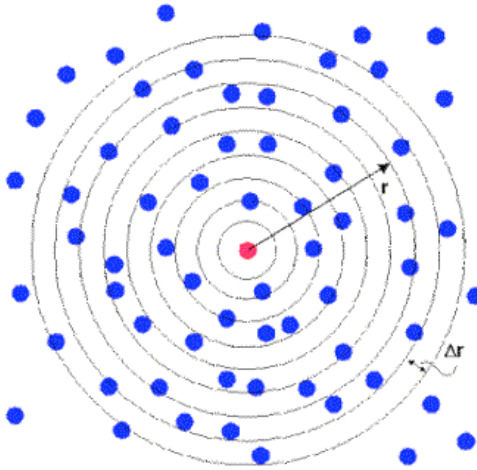


Figure 2. Schematic representation of how to calculate RDF functions.¹⁴

At regular intervals a snapshot of the system is taken and the number of atoms found in each shell is counted and stored. At the end of the simulation, the average number of atoms in each shell is calculated and then divided by both the volume of each shell and the average density of atoms in the system. The result is the radial distribution function. Mathematically the formula is,

$$g(r) = \frac{n'(r)}{\rho 4\pi r^2 \Delta r} \quad (1)$$

In equation (1), $n'(r)$ is the number of atoms in a shell of width Δr at a distance r and ρ is the atom density. The method need not be restricted to one atom. All the atoms in the system can be treated in this way, leading to an improved determination of the RDF as an average over many atoms. The radial distribution function is usually plotted as a function of the interatomic separation r .

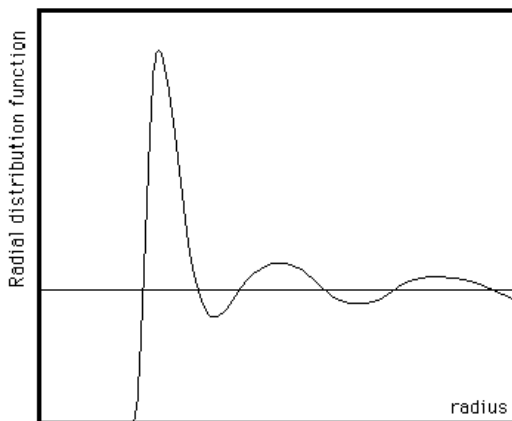


Figure 3. Radial Distribution Function, $g(r)$.¹⁴

A typical plot of a RDF (see Figure 3) shows a number of important features. Firstly, at short separations (small r) the RDF is zero. This indicates the effective width of the atoms, since they cannot approach any more closely. Secondly, a number of obvious peaks appear, which indicate that the atoms pack around each other in "shells" of neighbors. The occurrence of peaks at long range indicates a high degree of ordering. Usually, at high temperatures the peaks are broad, indicating thermal motion, while at low temperature they are sharp. They are particularly sharp in crystalline materials, where atoms are strongly confined in their positions. At very long range every RDF tends to a value of 1, which happens because the RDF describes the average density at this range.

X-ray and neutron diffraction experiments are standard measurements that provide information about pair correlation functions and, thus, the determination of $g(r)$ functions. For this reason, most of the potential energy models applied to MD simulations are tested by

comparing calculated and measured RDF functions.^{5,12,15} In particular, the ABEEM ammonia-8P model¹² has been applied to an ensemble of 256 molecules of ammonia and the calculated RDFs have been compared with experimental measurements.¹² Moreover, Boese et al.⁵ calculated the N-N, H-H and N-H RDFs from the atomic trajectories generated by ab initio molecular dynamics simulations using the Car-Parrinello method.¹⁶ In both studies, no comparisons with other experimental properties, such as density, are performed. However, density at different temperatures and mean diffusion coefficients are interesting properties to visualize the interval of temperatures at which a phase change is likely to occur.

The mean value of $n(r)$, representing the number of atoms (or molecules) in the first solvation shell, the so-called coordination number, $n(r)$, can be determined by integrating the $g(r)$ function to the first minimum

$$n(r) = \int_{r_1}^{r_2} 4\pi r^2 \rho g(r) dr \quad (2)$$

Well defined coordination numbers are indicative of an ordered structure. However, the coordination number of systems with disorder cannot be precisely defined. In case of well structured first solvation shells, the coordination number represented at different values of the distance presents a clear plateau, as shown in Figure 4.

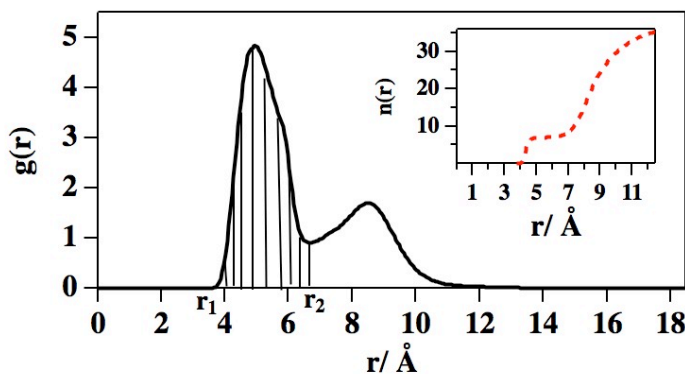


Figure 4. Integration of the first peak of $g(r)$ giving the coordination number.

In addition to the structural data mentioned above, MD simulations provide other properties of the systems as for instance density and mean diffusion coefficients, interesting properties due to their different values in gas and in condensed phases. Variations of the density can be calculated from the number of particles and the volume of the box containing the system and this requires MD simulations allowing the box to expand or to contract. The mean diffusion coefficients are estimated from the displacement of the particles along the simulation time applying the Einstein law which indicates that the square of the distance between a particles initial site at $t = 0$ and that to later time is proportional to the travel time t (at large times),³

$$D = \lim_{t \rightarrow \infty} \frac{\sum_{i=1}^N (\vec{r}_i(t) - \vec{r}_i(0))^2}{6Nt} \quad (3)$$

4. OBJECTIVES

The main objectives of the present study are:

a) The formulation of the $\text{NH}_3\text{-NH}_3$ non electrostatic intermolecular interaction, justifying the choice of the analytical function and giving the parameterization details.

b) The prediction of binding energies and equilibrium geometries for the $(\text{NH}_3)_{2-5}$ small clusters by carrying out Molecular Dynamics simulations using the NVE ensemble.

c) The prediction of densities and mean diffusion coefficients for liquid ammonia in a range of temperatures.

d) The determination of structural properties for liquid ammonia by computing radial distribution functions and coordination numbers.

e) Comparison of the predicted results with experimental and ab initio data.

5. THE $\text{NH}_3\text{-NH}_3$ INTERMOLECULAR INTERACTION

In MD simulations, the calculation of the force acting on every particle is the most time consuming part of the simulation and the use of pairwise additive interactions, described by means of simple analytical functions, with analytical and continuous derivatives, should allow a diminution of the computational cost of the simulation. Obviously, the quality of the MD results depends on the accuracy of the function and the reliability of the corresponding parameters defining the force field. The formulation of the total potential energy function describing the intermolecular interaction, V , needs the consideration of long ranged and short ranged contributions. Usually, in MD simulations it is assumed that the pair-body terms arise from van der Waals (V_{nel}) and/or electrostatic (V_{el}) forces. The former are regarded as short ranged while the latter are considered long range forces. The different characteristics of these forces justify their separability, which is often assumed in MD simulations. Accordingly,

$$V=V_{nel}+V_{el} \quad (4)$$

The calculation of the weak interactions included in V_{nel} is difficult and considerable attention has been given to the search of adequate potential energy functions of sufficiently general validity.¹⁷

In the present study, V_{nel} is formulated by means of an Improved Lennard Jones function (V_{ILJ}),^{18,19} which adds flexibility to the well known Lennard Jones one (V_{LJ})²⁰ and, at the same time, removes most of its inadequacies. The main differences between both potential energy functions are analysed in the next sections.

5.1 THE LENNARD JONES FUNCTION

The Lennard Jones function, based on the assumption of the pairwise atom–atom-like additivity of the interaction potential energy, is one of the most used in MD simulations and it is expressed by,

$$V_{LJ} = \varepsilon \left[\left(\frac{r_m}{r} \right)^{12} - 2 \left(\frac{r_m}{r} \right)^6 \right] \quad (5)$$

where r , represents the distance from two interaction centres and ε and r_m are adjustable parameters related with the well depth and the intermolecular distance at the minimum of the potential energy. Moreover, r_m is related with σ , the value of the distance at which V_{LJ} is equal to zero. As an example, the Lennard-Jones potential for $O(^3P)$ -He system, indicating the meaning of the parameters, is shown in Figure 5.

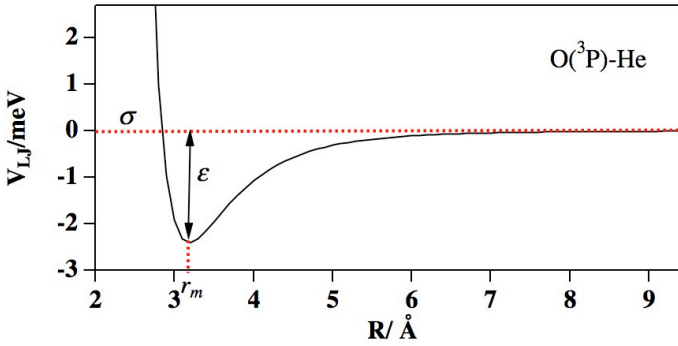


Figure 5. Lennard-Jones potential energy for the $O(^3P)$ -He system.

The LJ function, although satisfactorily reproduces the features of the potential well, exhibits known limits in describing both the short range repulsion and the long range attraction. In particular, it is too repulsive at short-range and asymptotically overestimates the attraction as much as a factor of two.

5.2. THE IMPROVED LENNARD JONES FUNCTION

The Improved Lennard Jones function is represented by,

$$V_{ILJ} = \varepsilon \left[\frac{m}{n(r) - m} \left(\frac{r_m}{r} \right)^{n(r)} - \frac{n(r)}{n(r) - m} \left(\frac{r_m}{r} \right)^m \right] \quad (6)$$

In the equation (6), the parameters ε and r_m have the same meaning as before. However, in the ILJ function the exponent of the repulsive part of the potential energy function is not a constant as in the LJ function, but a function of the distance,

$$n(r) = \beta + 4.0 \left(\frac{r}{r_m} \right)^2 \quad (7)$$

where β is an adjustable parameter, depending on the nature and hardness of the interacting particles. For neutral-neutral systems, for which $m=6$, β can take values in the 6.5 - 11 range, whereas for ion-neutral systems for which $m=4$, β can take lower values.^{18,21} By modifying the value of β it is possible to use the same values of the relevant parameters (having a physical meaning) of the potential function (ε and r_m) in different environments. Accordingly, the β parameter adds flexibility to the ILJ function with respect to the LJ one. Moreover, in comparison with the LJ function, the repulsive and the attractive part of the ILJ function become less repulsive and less attractive, respectively. The ILJ model is computationally simple, also regarding its derivatives, and it is defined in practice by only two parameters (for a given system β is a constant). Moreover, it is capable to cover an ample phenomenology of interactions, such as neutral-neutral systems ($m=6$), ion-neutral systems ($m=4$), etc.

5.3. THE PARAMETERS OF THE IMPROVED LENNARD JONES FUNCTION

The property basically responsible for van der Waals forces is the polarizability. Polarizability allows us to better understand the interactions between nonpolar atoms and molecules and other electrically charged species, such as ions or polar molecules with dipole moments. In fact, polarizability determines the long range dispersion. Moreover, since polarizability is related mainly to the size of the outer electronic orbitals, it can also be taken as a measure of the repulsion (at least in a range near the equilibrium distance). Bearing in mind that an interaction potential is due to a combined effect of repulsive and attractive contributions, the polarizability has been used to calculate the ε and r_m parameters of the ILJ potential energy function.²² For two A and B neutral systems (atoms or molecules), r_m (in Å) is calculated as follows,

$$r_m = C \frac{\alpha_A^{1/3} + \alpha_B^{1/3}}{(\alpha_A \alpha_B)^\gamma} \quad (8)$$

where α represents the polarizability (in \AA^3). The numerator represents the effect due to the atomic size and the denominator the effect due to the attraction. The C coefficient and the exponent γ , equal to 1.767 and 0.095, respectively, have been obtained as an average of different values using well known systems such as Ne-Ne, Ne-Ar and He-Ar. On the other hand, ε can be obtained by considering the near proportionality $\varepsilon \propto C_{6\text{eff}} r_m^{-6}$.

For two neutral systems, following the same procedure used to formulate r_m , ε can be calculated from,

$$\varepsilon = 0.720 \frac{C_{6\text{eff}}}{r_m^6} \quad (9)$$

The $C_{6\text{eff}}$ constant is an effective long-range interaction term, which includes dipole-dipole, dipole-multipole and multipole-multipole interactions, which can be determined from scattering experiments.¹⁹ Such experiments have probed the dependence of $C_{6\text{eff}}$ on the polarizability of the interacting particles. In fact, $C_{6\text{eff}}$ can be determined from the following equation,

$$C_{6\text{eff}} = K \frac{\alpha_A \alpha_B}{\left(\frac{\alpha_A}{N_A}\right)^{1/2} + \left(\frac{\alpha_B}{N_B}\right)^{1/2}} \quad (10)$$

where N_A and N_B are the number of effective electrons of A and B respectively and $K=361.5$ to obtain $C_{6\text{eff}}$ values in $\text{kcal mol}^{-1} \text{\AA}^6$.

The number of effective electrons can be obtained from ab initio calculations by determining the relative perturbation induced by a point charge on the various atomic orbitals.²² However, in the absence of ab initio results it can be estimated from a first order approximation formula, for molecules made up by light atoms,

$$N_{\text{eff}} = N_t \left(1 - \frac{N_b N_{nb}}{N_t^2} \right) \quad (11)$$

where N_b and N_{nb} are the number of bonded electrons and that of the no bonded ones respectively and N_t is the sum of the two.

5.4. THE ILJ PARAMETERS FOR THE NH₃-NH₃ INTERACTION

The ε and r_m parameters of the ILJ potential energy function for the NH₃-NH₃ interaction have been calculated by considering two interaction centres placed on the N atoms of the molecules with an assigned polarizability equal to the molecular one ($\alpha_{\text{NH}_3} = 2.103 \text{ \AA}^3$). The NH₃ molecule has a total of 10 electrons, of which 6 take part in the bonds and 4 remain unbounded. Accordingly, using equation 11, $N_{\text{eff}} = 7.6$ and then, for the NH₃-NH₃ interaction, the equations (8) and (10) are expressed as,

$$r_m = 3.534(\alpha_{\text{NH}_3})^{0.1433} \quad \text{and} \quad C_{6\text{eff}} = 498.29(\alpha_{\text{NH}_3})^{1.5}$$

Finally, once the r_m and $C_{6\text{eff}}$ values have been determined, ε can be calculated by means of equation (9). The parameters defining the NH₃-NH₃ non electrostatic interaction are given in Table 1.

$r_m / \text{\AA}$	$\varepsilon / \text{kcal mol}^{-1}$	β	m
3.931	0.2965	6.7	6

Table 1. Parameters of the ILJ function for the NH₃-NH₃ interaction.

The choice of $b = 6.7$ seems to be adequate to describe the formation of hydrogen bonds. As a matter of fact, the value of 6.7 was also used to investigate some small clusters of rigid water molecules.^{23,24} On the other hand, the value of $m = 6$, as it has been indicated before, is the typical one for neutral-neutral interactions.

Regarding the electrostatic interaction, V_{el} , it has been calculated by assuming a four point charge distribution obtained at the MP2/aug-cc-pVDZ level, with charges of 0.3274 a.u. placed on the H atoms and of -0.9822 a.u. on the N atom.¹² This charge distribution is compatible with a dipole moment value of 1.64 D,¹² which is about 12% larger than that of NH₃ in the gas phase, equal to 1.47 D.²⁵ This choice is based on the fact that to investigate small water clusters we have used the well-determined dipole moment of the dimer equal to 2.1 D, which is about 13% higher than the dipole moment of water in the gas phase (1.85 D).

6. THE SMALL $(\text{NH}_3)_{2-5}$ AGGREGATES

To ensure the conservation of total energy (E_{tot}) a NVE ensemble of particles has been considered. E_{tot} is defined at each step of the simulation as the sum of the potential energy (E_{cfg}), calculated as indicated before, and the kinetic energy (E_{kin}). At the end of the simulation, the mean averages of temperature and of E_{cfg} are calculated. MD simulations for each aggregate have been performed at increasing values of T (and accordingly of E_{kin}), starting each new simulation from the last configuration of the previous run.

6.1. ESTIMATION OF THE $(\text{NH}_3)_{2-5}$ BINDING ENERGIES

An estimation of the binding energy can be obtained by extrapolating the mean values of E_{cfg} to $T=0$ K (see Figure 6). In previous studies it has been observed that when no isomerization takes place, the mentioned extrapolation predicts binding energies very close to those of the actual minimum (see for instance ref. 26).

In Figure (6), from left to right and from top to bottom, the different energies for the dimer, trimer, tetramer and pentamer obtained by means of MD simulations are represented as a function of T . The first point, represents the binding energy and, as it has been indicated above, is derived from the extrapolation to $T=0$ K of the lineal fit of the energy values as a function of T . The corresponding values of the binding energies for each ammonia aggregate are also given in Table 2.

$(\text{NH}_3)_n$	n=2	n=3	n=4	n=5
Binding Energy (Kcal/mol)	2,47	7,29	11,54	14,90

Table 2. Binding energy values of $(\text{NH}_3)_{2-5}$ aggregates obtained by extrapolation of E_{cfg} to $T=0$ K.

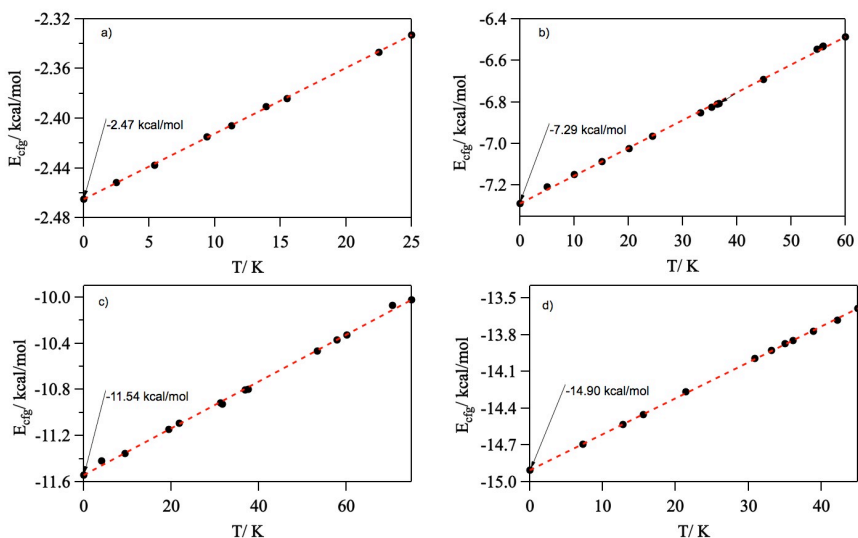


Figure 6. E_{cfg} values obtained at several temperatures. The discontinuous line corresponds to the linear fit of the energy values at the different temperatures. $(\text{NH}_3)_2$ and $(\text{NH}_3)_3$ on the top (left and right hand side, respectively). $(\text{NH}_3)_4$ and $(\text{NH}_3)_5$ on the bottom (left and right hand side, respectively).

As regarding the dimer binding energy, the estimated value of 2.47 kcal/mol is in a quite good agreement with *ab initio* and experimental results. Values between 3.15 kcal/mol and 1.81 kcal/mol are reported in the literature.⁵ However, typical theoretical values of the binding energy are close to 3 kcal/mol (see for instance ref. 12), without the zero point energy correction. The comparison of the experimental values of D_0 found in the literature, equal to 1.89 kcal/mol (661 cm^{-1})⁵ and 1.62 kcal/mol (567 cm^{-1}),⁹ with the predicted value of 2.47 kcal/mol suggests a zero point energy correction in the 31%-52% range, in agreement with the proposed value of the zero point energy, equal to a 42% of the binding energy.¹⁰ The value of 2.47 kcal/mol is in the lower limit of binding energies given in the literature for the dimer. It must be taken into account, however, that the agreement could be easily improved by slightly modifying the NH_3 charge distribution. In the present study, as it has been indicated before, we have considered the charge distribution calculated at the MP2/augcc-pVDZ level, which corresponds to an increase of the dipole moment of the NH_3 monomer similar to that used for H_2O and which has been used in other theoretical calculations.¹² Binding energy of the remaining clusters is slightly lower than the reported values found in the literature. The calculated values of the trimer binding

energy fall in the 8.2-10.0 kcal/mol interval. Values in the 12.6-15.5 kcal/mol range are found for the tetramer.²⁷ The values of the pentamer binding energy found in the literature are in the 16.72-19.4 kcal/mol interval,²⁷ indicating a higher stability than the predictions of the potential model.

6.2. QUASI-LINEAR AND BENT NH...N CONTACTS

The configuration obtained at the lowest T investigated for each aggregate is very close to the equilibrium one and allows performing an estimation of the geometrical parameters for each cluster. The corresponding equilibrium-like configurations are shown in Figure 7.

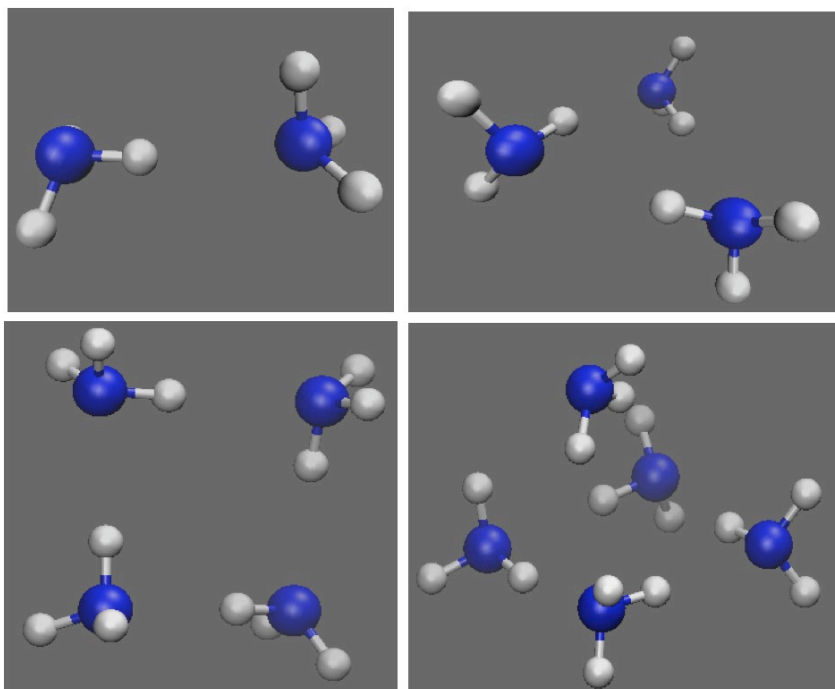


Figure 7. $(\text{NH}_3)_{2-5}$ equilibrium-like structures obtained from MD simulations at 10 K.

For the $(\text{NH}_3)_{2-4}$ clusters quasi-linear $\text{HN}\dots\text{H}$ contacts are preferred to the bent ones. Nevertheless, the $(\text{NH}_3)_5$ cluster presents also some bent hydrogen bonds.

In order to analyse better the different kind of contacts, the behaviour of the ammonia dimer along the trajectories has been exhaustively investigated at several temperature values.

As it has been indicated before, H-bonded and cyclic structures have been proposed for the ammonia dimer. These structures have very similar binding energies, being the H-bonded structure only 7 cm^{-1} stabler than the cyclic one. The small difference on the binding energies of the different isomers makes difficult to detect the less stable structure from MD simulations. In spite of this, and in order to determine the beginning of isomerization processes, an exhaustive analysis of the evolution of the 6 $\text{N}\dots\text{H}$ intermolecular distances and of the six NHN angles along the simulation time has been performed for the ammonia dimer. When no isomerization occurs, small oscillations on the $\text{N}\dots\text{H}$ intermolecular distances, r_{NH} , are observed. On the contrary, an isomerization process causes important variations on the values of the intermolecular distances.

Due to the small barriers connecting different isomers, isomerizations are usually observed at very low values of T . Often, the structures before and after the isomerization processes are equivalent. MD simulations have shown that $(\text{NH}_3)_2$ isomerize at temperatures of about 28 K . Frequent changes on the values of the six r_{NH} distances are observed, as shown in Figure 8, where the evolution of the distances along the simulation time are represented.

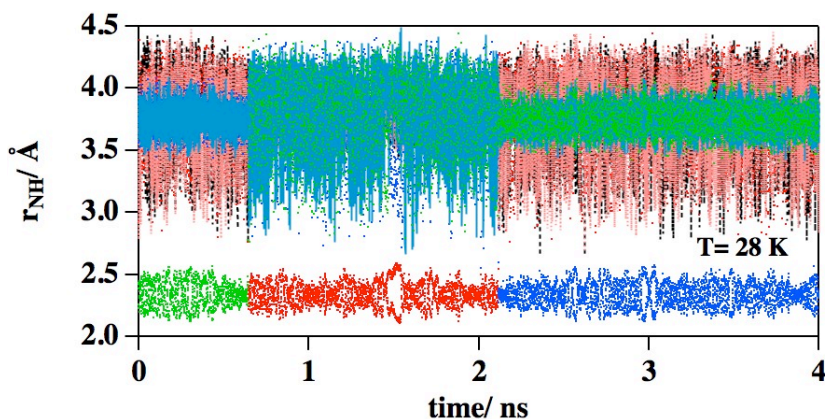


Figure 8. Evolution of the intermolecular r_{NH} distances for $(\text{NH}_3)_2$ along a trajectory obtained from MD simulations at 28 K .

The distance evolution shown in Figure 8 is indicative of isomerization processes. However, as indicated above, since the different isomers have very similar energies, their identification is very difficult.

As a matter of fact, as it can be seen in Figure 9 where the potential energy values along the simulation time are represented for the ammonia dimer, the fluctuations of E_{cfg} are only about 0.25 kcal/mol, which could be indicative of isomerizations from linear to cyclic structures.

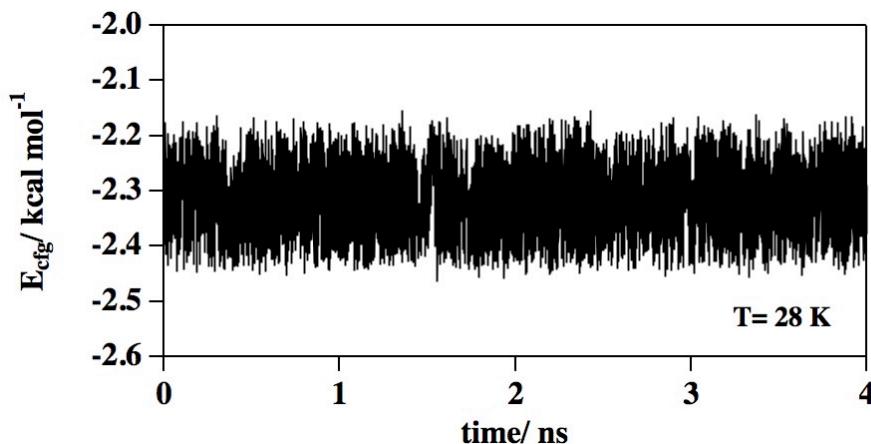


Figure 9. Evolution of the intermolecular potential energy for $(\text{NH}_3)_2$, E_{cfg} , along a trajectory obtained from MD simulations at 28 K.

In order to analyse the presence of cyclic structures along the trajectory, the evolution of the NH distances and of the N...HN angles have been further investigated. In particular, in Figure 10 the evolution on one of the r_{NH} distances and on one of the N...HN angles along the simulation time, obtained from MD simulations performed at 28 K, are represented.

The analysis of the configurations attained along the trajectory reveals that most of the geometries correspond to H-bonded configurations. Cyclic structures are also observed but they tend to isomerize quickly. This behaviour is reflected in Figure 10.

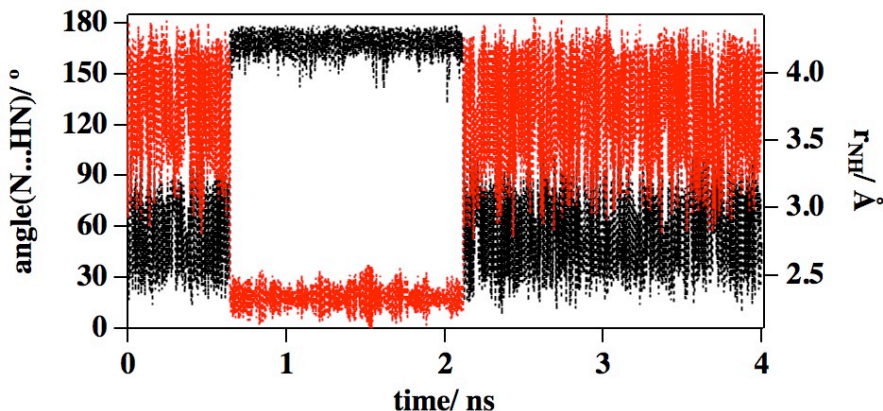


Figure 10. Evolution of the intermolecular r_{NH} distance (in red) and of the corresponding N...HN angle (in black) along a trajectory obtained from MD simulations at 28 K.

In Figure 10 it is also reflected the high stability of the H-bonded structure, the configuration associated to the minimum energy, for which only small variations of the angle and distance are observed for about 1.5 ns (from a time of 0.65 ns to 2.11 ns).

In order to analyse better the dimer structures, the distribution of the angles α and β , defining the orientation of the axes of the NH_3 molecules with respect to the intermolecular axis, represented in Figure 11, has been analyzed.

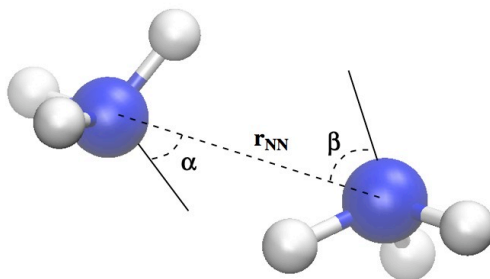


Figure 11. Ammonia dimer orientation angles (α and β).

The distribution of the orientation angles α and β at 28 K of temperature are shown in Figure 12, where it can be observed that the maximum of the distribution is about 30° and 115° for the α and β angles respectively, being the mean r_{NN} distance of 3.290 \AA . These values are in good agreement with the high-resolution rotational spectra, which found a r_{NN} distance of 3.366 \AA and α and β angles of 48.6° and 115.5° respectively.²⁸

The angle distributions indicate that both quasi-linear and cyclic structures are present along the trajectory. This fact, together with the small fluctuation of E_{cfg} along the trajectory seems to indicate that isomerizations between cyclic and quasi-linear structures are likely to occur, in agreement with the fact that ammonia dimer is a fluxional molecular complex.⁴ The same behaviour has been also observed for trimer and tetramer.

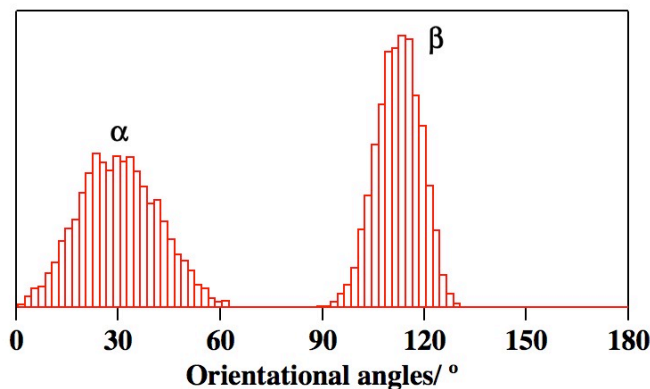


Figure 12. Distribution of the orientation angles α and β for the ammonia dimer obtained from MD simulations at 28 K.

In Table 3 are given certain other properties of structure as the N-N distance between different molecules in the aggregates, and the angle between a molecular bond and the formed H bond, angle (NH...N), which is an important property as the structure is due to this interaction.

$(\text{NH}_3)_n$	n=2	n=3	n=4
distance N-N/ \AA	3.29	3.30 ± 0.05	3.26 ± 0.01
angle(NH...N)/ $^\circ$	173	167 ± 2	177 ± 1

Table 3. Estimated values of the N-N distance and NH...N angle of $(\text{NH}_3)_{2-4}$ equilibrium-like structures obtained from MD simulations at 10 K.

We can define a unique (with a small variation) N-N distance and angle (NH...N) for the dimer, trimer and tetramer because the H-bonds in these aggregates are very similar, consequence of its particular geometry. However, the pentamer has a particular molecular distribution (see Figure 13).

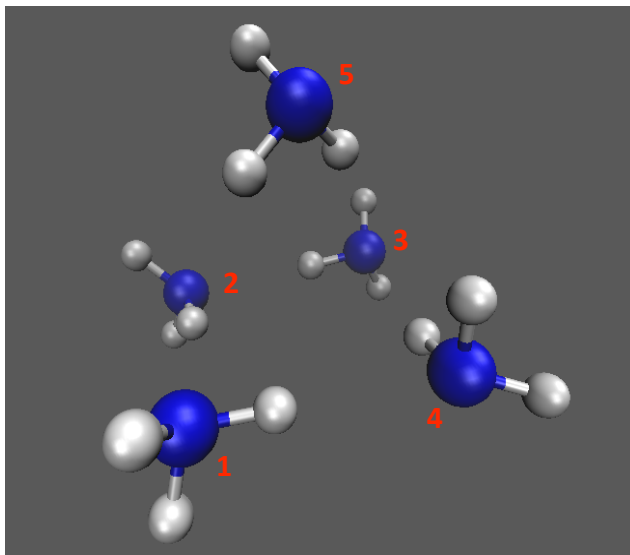


Figure 13. $(\text{NH}_3)_5$ equilibrium structure obtained from MD simulations at 10K.

$(\text{NH}_3)_5$	2-1	3-2	4-3	1-4	5-1	5-3
distance N-N/ Å	3.26	3.26	3.36	3.24		
angle(NH...N)/ °	172	175	164	179	155	159

Table 4. $(\text{NH}_3)_5$ equilibrium structure obtained from MD simulations at 10K.

If we compare the geometry of the tetramer with that of the four ammonia molecules on the pentamer (having the N atoms placed in the same plane), we can observe some differences. Three of the N-N distances are of the same order of magnitude that those found for the tetramer, but the fourth, equal to 3.36 Å, is a little bit larger. This fact can be explained because the fifth NH_3 molecule placed above the tetramer participates in two hydrogen bonds, with its

pair of electrons pointing towards one of the ammonia molecules, which tend to be placed at larger distances. As it is shown in Figure 13, the pair of electrons of ammonia 5 forces ammonia 4 to move away, thus increasing the N-N distance with respect that of the regular tetramer. We can also observe that ammonia 5 participates in two weak hydrogen bonds with ammonia 1 and 3 and this is reflected in the hydrogen bonds formed between ammonia 2 and 1, on one hand, and ammonia 4 and 3, on the other, which are weaker, originating a diminution of the (NH...N) angle (bent contacts).

7. LIQUID AMMONIA

The initial configuration to investigate liquid ammonia has been constructed by a random distribution of 512 molecules of NH_3 placed into a cubic box of 31.64 Å of length. At first, in order to describe the ammonia density at a given T , the system has been thermalized using the NVT ensemble of particles. Once the temperature of the system has been equilibrated, MD simulations have been performed at constant values of the number of molecules, N ; pressure, p ; and temperature, T (NpT ensemble). The effect of increasing T has been analysed at constant values of N and p . The use of an NpT ensemble, allows the box freely expand or contract and variations on the values of the density (d) can be analysed.

Following the same procedure used to investigate liquid water, the dipole moment value of the monomers has been increased in about a 14 % and punctual charges of -1.08042 a.u. and 0.36014 a.u have been placed on the N and H atoms, respectively. As it has been indicated for water, in the condensed phases the self-consistent internal electric field polarizes the molecules, leading to a large increase of the dipole moment.^{29,30}

7.1. DENSITY AND MEAN DIFFUSION COEFFICIENTS

The results obtained at the 220 K - 350 K range of temperatures have been analysed. In Figure 14, the behavior of both density (top panel) and approximate mean diffusion coefficient (D , lower panel) values are represented for the temperature range investigated. A gradual decrease of the density is observed when increasing T , and at $T= 239.8$ K the density of liquid ammonia is equal to 0.699 g/cm³. This value is only a 2.5 % larger than the experimental value, 0.682 g/cm³ at the boiling point ($T_{\text{boiling}}= 239.82$ K). As it can be seen in the figure, the density modifies its dependence on T around $T=250$ K, which can be attributed to a phase change.²⁶ In

spite of the fact that this change is less evident for the mean values of the diffusion coefficients, it is also observed.

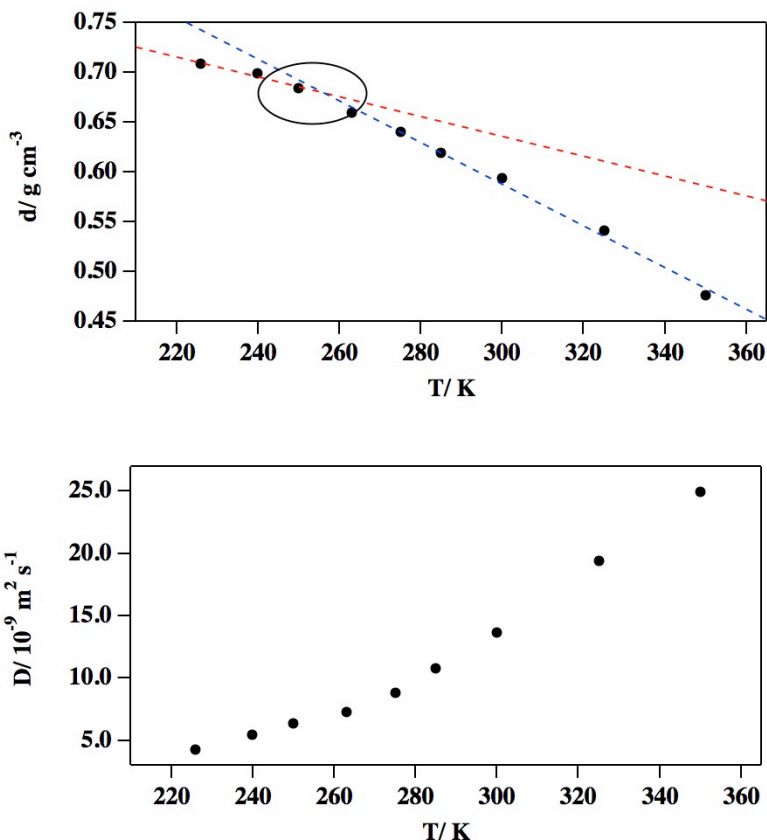


Figure 14. Density (top panel) and approximate mean diffusion coefficients (lower panel) as a function of the temperature at $p=1\text{atm}$.

7.2. RADIAL DISTRIBUTION FUNCTIONS AND COORDINATION NUMBERS

Structure of liquid ammonia has been also investigated and the N-N, the H-H and the N-H RDFs, represented by $g(r_{\text{NN}})$, $g(r_{\text{HH}})$ and $g(r_{\text{NH}})$, respectively, have been calculated at several values of the temperature. Moreover, the coordination number, represented by $n(r)$, has also been calculated. In particular, in Figure 15 the N-N radial distribution function (black continuous

line) and the coordination number (red discontinuous line) obtained at 275 K are shown. As it can be seen, the first peak on $g(r_{\text{NN}})$ is unstructured, although slightly asymmetric on the high r values side. The position of the minimum after the first peak is close to 5.2 Å, being the coordination number at this distance equal to 13. The second peak is roughly twice the position of the first peak, which together with a coordination number of 13, suggest a close packing in the ammonia molecules. These results are in good agreement with those derived from neutron diffraction experiments at 277 K at a pressure of 0.48 atm.¹⁴ In particular, the N-N RDF predicted by our potential model starts to be detected at 2.6 Å, as was observed in ref. 14. The position of the first and second peaks, centred at 3.425 Å and 6.725 Å respectively, are also in good agreement with the neutron diffraction results of Ricci et al.¹⁴ Moreover, these authors found a coordination number of about 14.

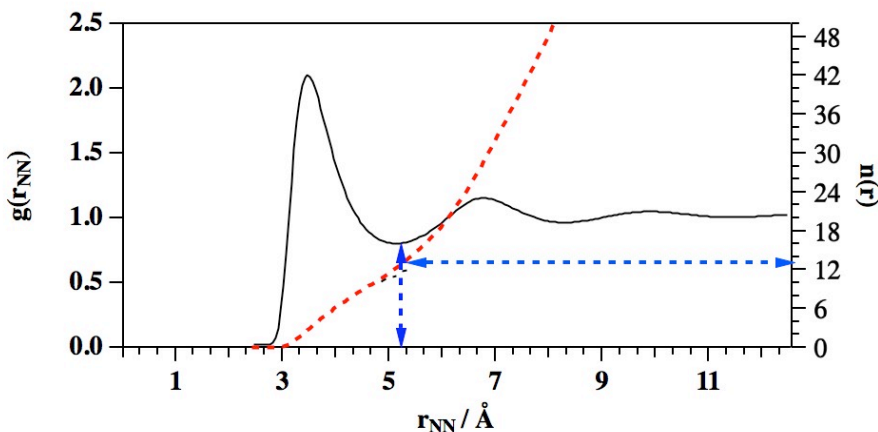


Figure 15. The N-N RDF, $g(r_{\text{NN}})$, and the coordination number, $n(r)$, obtained from MD simulations at $T=275$ K and $p=4.8$ atm.

The positions of the peaks are also in agreement with the values derived from X-ray experiments.¹³ In spite of the fact that X-ray experiments found more structured peaks on the $g(r_{\text{NN}})$ function, it has been attributed as artefacts of the data analysis.¹⁴ The corresponding coordination number derived from X-ray diffraction experiments is equal to 12.

The obtained results are also in agreement with those derived from the more complex interaction potential,¹² which describes a $g(r_{\text{NN}})$ function showing an asymmetric first peak centred at 3.35 Å, followed by a minimum placed at 4.62 Å. The $g(r_{\text{NN}})$ function using the ABEEM ammonia-8P potential model has been applied to an ensemble of 256 NH₃ molecules and shows a first peak with a height close to 2.2 placed at 3.35 Å and a much more structured $g(r_{\text{NN}})$ at large distances in comparison with the available experimental data. On the other hand, Boese and collaborators,⁵ performed Car-Parrinello ab initio MD simulations using two different density functionals, one of them constructed to describe accurately the hydrogen ammonia bond in the ammonia dimer. Results indicate that the first peak is located at a distance of about 0.15 Å larger than the experimental peak derived from neutron diffraction experiments. However, the overall shape of the first peak is well represented and when the N-N RDF is integrated up to their first minimum, a value of 13.2 is obtained, in agreement with the value obtained using the ILJ function.

The $g(r_{\text{NH}})$ and the $g(r_{\text{HH}})$ functions, together with the corresponding coordination numbers are represented in the top and lower panels of Figure 16, respectively.

In the top panel, where the N-H RDF is represented, it can be seen, in agreement with experimental results, a shoulder up to about 2.6 Å and a more pronounced peak at the larger distance at around 3.7 Å. This structure is due to the presence of H-bonded and non-H-bonded atoms in the first solvation shell. Considering both hydrogen bonded and non-hydrogen bonded H atoms, a sphere of radius 5.2 Å around N is found. The integration of the $g(r_{\text{NH}})$ function up to the distance of 5.2 Å indicates that the number of H atoms around a central N belonging to a different molecule is of the order of 39, in agreement with the previous finding of 13 molecules of NH₃ in the same range of distances.

In the lower panel, the $g(r_{\text{HH}})$ function, in agreement with ab initio calculations^{3,11} and experimental results,^{12,13} exhibits a slightly pronounced first solvation shell with a small hump close to 3.7 Å. The calculated coordination number, defined here as the number of H atoms around a central H belonging to a different molecule is, as expected, equal to 39.

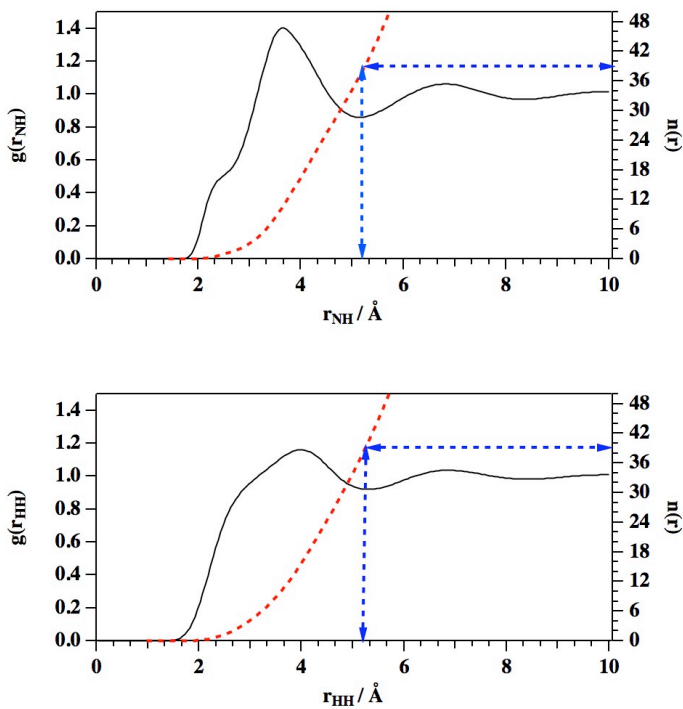


Figure 16. N-H and H-H RDFs, $g(r_{\text{NH}})$ (top panel) and $g(r_{\text{HH}})$ (lower panel) and coordination numbers, $n(r)$ obtained from MD simulations at $T=275$ K and $p=4.8$ atm.

8. CONCLUSIONS

The potential energy function used to describe the non electrostatic contribution of the intermolecular energy has been parameterized using the value of the molecular polarizability of NH_3 . The potential energy function, combined with the electrostatic contribution of the energy calculated by assuming a four point charge distribution has been applied to study both, some small ammonia clusters and liquid ammonia by means of Molecular Dynamics simulations.

It has been proved that the microcanonical ensemble of particles (NVE) is suitable to study the small ammonia clusters.

The small clusters of ammonia tend to isomerize at very low temperatures.

Different contacts between ammonia molecules, H-bonded and bent, have been observed in the small clusters.

Geometries and binding energies for the small clusters are in a quite good agreement with experimental and ab initio data found in the literature.

The values of the binding energy are in the lower limit of the published data, which can be attributed to the fact that in MD simulations the bent configurations, less stable than the linear ones, are also explored. However, a complete agreement with the best-published results could be achieved by slightly modifying the electronic charge distribution on the molecule.

An increase of about a 14 % (very similar to that applied for liquid water) of the dipole moment of the ammonia used to investigate the small clusters seems to be adequate to study liquid ammonia.

It has been proved that isothermal and isobaric simulations (NpT) are suitable to determine both bulk and structural properties of liquid ammonia.

Simulations at increased values of T allow observing the tendency of the system to pass from liquid to gas phase.

Structural properties of the liquid have been investigated and the obtained radial distribution functions and the coordination number are in very good agreement with results of X-ray and neutron diffraction experiments.

All the obtained results seem to corroborate that the molecular polarizability of NH_3 is a good property to describe the non electrostatic intermolecular interaction in both gas (small clusters) and liquid phase.

9. REFERENCES AND NOTES

1. Engin C.; Merker T.; Vrabc J.; Hasse H.; Flexible or rigid molecular models? A study on vapour-liquid equilibrium properties of ammonia. *Mol. Phys.* **2011**, *109*, 619-624.
2. B. Eckl, J.Vrabc and H. Hasse, An optimised molecular model for ammonia. *Mol. Phys.* **2008**, *106*, 1039-1046.
3. Ikeda K., On the Theory of Isothermal-Isobaric Ensemble. I. *Progr. Theoret. Phys.* **1967**, *38*, 3.
4. Boese, A.D.; Chandra, A.; Martin, J.M.; Marx, D. From ab initio quantum chemistry to molecular dynamics: The delicate case of hydrogen bonding in ammonia. *J. Chem. Phys.* **2003**, *119*, 5965-5980.
5. Case, A.S.; Heid, G.C.; Kable, S.H.; Crim, F.F. Dissociation energy and vibrational predissociation dynamics of the ammonia dimer. *J. Chem. Phys.* **2011**, *135*, 084312(1)- 084312(9).
6. Bacic, Z.; Buck, U.; Meyer, H.; Shinke, R. Energy transfer in ammonia-dimer-helium collisions. *Chem. Phys. Lett.* **1986**, *125* 47-52.
7. Snels, M.; Fantoni, R.; Sanders, R.; Meerts, W.L. IR dissociation of ammonia clusters. *Chem. Phys.* **1987**, *115*, 79-91.
8. Slipchenko, M.N.; Sartakov, B.G.; Vilesov, A.F.; Xantheas, S.S. Study of NH Stretching Vibrations in Small Ammonia Clusters by Infrared Spectroscopy in He Droplets and ab Initio Calculations. *J. Phys. Chem. A.* **2007**, *111*, 7460-7471.
9. Altmann, J.A.; Govender, M.G.; Ford, T.A. *Ab initio* and DFT calculations of some weakly bound dimers and complexes. I. The dimers of ammonia and phosphine. *Mol. Phys.* **2005**, *103*, 949- 961.
10. Curotto, E.; Mella, M. Quantum Monte Carlo simulations of selected ammonia clusters ($n = 2-5$): Isotope effects on the ground state of typical hydrogen bonded systems. *J. Chem. Phys.* **2010**, *133*, 214301(1)- 214301(16).
11. Yu, L.; Yang, Z-Z. Study on structures and properties of ammonia clusters $(\text{NH}_3)_n$ ($n=1-5$) and liquid ammonia in terms of ab initio method and atom-bond electronegativity equalization method ammonia-8P fluctuating charge potential model. *J. Chem. Phys.* **2010**, *132*, 174109(1)- 174109(11).
12. Narten, A.H. Liquid ammonia: Molecular correlation functions from X-ray diffraction. *J. Chem. Phys.* **1977**, *66*, 3117-3120
13. Ricci, M.A.; Nardone, M.; Ricci, F.P.; Andreani, C.; Soper, A.K. Microscopic structure of low temperature liquid ammonia: A neutron diffraction experiment. *J. Chem. Phys.* **1995**, *102*, 7650-7655.
14. http://www.ccp5.ac.uk/DL_POLY/Democritus/Theory/rdf.html
15. Car, R.; Parrinello, M (1985). Unified Approach for Molecular Dynamics and Density-Functional Theory. *Physical Review Letters* **1985**, *55*, 2471-2474.
16. Frenkel, D.; Smit, B. Understanding Molecular Simulations: From algorithms to applications. *Academic Press* (2nd edition), **2002**.
17. Halgren, T.A. Potential energy functions. *Current Opinion in Structural Biology.* **1995**, *5*, 205-210
18. Pirani, F. Alberti, M.; Castro, A.; Moix Teixidor, M.; Cappelletti, D. Atom-bond pairwise additive representation for potential energy surfaces. *Chem. Phys. Lett.* **2004**, *394*, 37-44.
19. Pirani, F.; Brizi, S.; Roncaratti, L.F.; Casavecchia, P.; Cappelletti, D.; Vecchiocattivi, F. Beyond the Lennard-Jones model: a simple and accurate potential function probed by high resolution scattering data useful for molecular dynamics simulations. *Phys. Chem. Chem. Phys.* **2008**, *10*, 5477-5640.
20. Lennard-Jones, J. E. Cohesion. *Proceedings of the Physical Society* **1931**, *43*, 461-482.
21. Alberti, M.; Castro, A.; Laganà, A.; Moix, M.; Pirani, F.; Cappelletti, D. Steric and energetic properties of the Cl-C6H6-Arn heterocluster. *Eur. Phys. J. D.* **2006**, *38*, 185-191.

22. Cambi, R.; Cappelletti, D.; Liuti, G.; Pirani, F. Generalized correlations in terms of polarizability for van der Waals interaction potential parameter calculations *J. Chem. Phys.* **1991**, *95*, 1852-1860.
23. Alberti, M.; Aguilar, A.; Cappelletti, D.; Laganà, A.; Pirani, F. On the development of an effective model potential to describe water interaction in neutral and ionic clusters. *Int. J. Mass. Spec.* **2009**, *280*, 50-56.
24. Alberti, M.; Faginas-Lago, N.; Laganà, A.; Pirani, F. A Portable Intermolecular Potential for molecular dynamics studies of NMA-NMA and NMA-H₂O aggregates. *Phys. Chem. Chem. Phys.* **2011**, *13*, 8422-8432.
25. NIST Data Base (<http://cccbdb.nist.gov/>).
26. M. Alberti, A. Aguilar, J.M. Lucas, F. Pirani. Competitive role of the CH₄-CH₄ and CH- π interactions in C₆H₆-(CH₄)_n aggregates: The transition from dimer to cluster features. *J. Phys. Chem. A.*, **2012**, *116*, 5480-5490.
27. Janeiro-Barral, E. P.; Mella, M.; Curotto, E. Structure and Energetics of Ammonia Clusters (NH₃)_n (n=3-20) investigated using a rigid-polarizable model derived from ab initio calculations. *J. Phys. Chem. A* **2008**, *112*, 2888-2898.
28. Slipchenko, M.N.; Sartakov, B.G.; Vilesov, A.F.; Xantheas, S.S. Study of NH stretching vibrations in small ammonia clusters by infrared spectroscopy in He droplets and ab Initio calculations. *J. Phys. Chem. A.* **2007**, *111*, 7460-7471.
29. Silvestrelli, P.L.; Parrinello, M. Water molecule dipole in the gas and in the liquid phase. *Phys. Rev. Lett.* **1999**, *82*, 3308-3311.
30. Gregory, J.K.; Clary, D.C.; Liu, K.; Brown, M.G.; Saykally, R.J. The water dipole moment in water clusters. *Science* **1997**, *275*, 814-817.

10. ACRONYMS

ABEEM ammonia-8P Atom Bond Electronegativity Equalization Method (used to calculate electrostatic charge distribution)

ILJ Improved Lennard Jones

LJ Lennard Jones

MD Molecular Dynamics

MP2/aug-cc-pVDZ, MP2/aug-cc-pVTZ Second order of the perturbation theory to calculate electronic correlation effects with two basis set type

NVE Microcanonical Ensemble

NpT Isobaric-Isothermal Ensemble

RDF and g(r) Radial Distribution Function

APPENDICES

APPENDIX 1: DL_POLY_2 FILES

For MD simulations we use the DL_POLY_2. This appendix describes all the input files for this programme. It generates also some output files, but as each MD simulation contain about 5 million steps, the OUTPUT files are too much long to be explained here.

In normal use, DL_POLY_2 requires three input files named CONTROL, CONFIG and FIELD.

The CONTROL file defines the control variables for running a DL_POLY_2 job.

```
NH3_n                                NH3_liquid

temperature 60.00                    temperature 275.00
pressure    0.001                    pressure    0.001
ensemble nve                                ensemble npt berendsen 0.100
2.0000

steps          5000000                steps          5000000
equilibration 999999                 equilibration 999999
scale          10                     scale          10
restart scale                                restart scale
print          1000                   print          1000
stack          1000                   stack          1000
stats          500                    stats          500
rdf            10                     rdf            10

timestep      0.0010                 timestep      0.0010
cutoff        15.5                   cutoff        12.5
delr width    1.2                    delr width    1.2
coul

quaternion tolerance 1.0000E-05    quaternion tolerance 1.0000E-05
#ewald precision 1.0E-5              ewald precision 1.0E-5
shake tolerance 1.0E-5              shake tolerance 1.0E-5
print rdf

#no vdw
print rdf

traj 1000000 500 0                  traj 1000000 500 0
job time 10000000.0                 job time 10000000.0
close time 150.0                    close time 150.0

finish                                finish
```

The CONFIG file contains the dimensions of the unit cell, the key for periodic boundary conditions and the atomic labels, coordinates, velocities and forces.

```

NH3_3
      2      0  5000000  0.1000000000E-02
N      1
  -0.6643276308      1.339626140      3.865189459
 -0.489551580232  0.368312704822      1.80030300697
 -1640.91490286  4205.27112580      3813.66520117
H      2
  -1.616628860      1.009193720      3.770193749
  0.128900000244  -1.03187481133  0.470928743873
  469.856170369  -817.635564248  -390.821891185
H      3
  -0.3412764107      1.036932978      4.775687639
  0.511607749608  -3.79295475039  0.616801538544E-01
  99.6305847193  -662.008950433  -431.700300134
H      4
  -0.1130905379      0.8380645494      3.179940732
  0.213451367026  5.08639533264  -1.08753559336
  817.874311832  -2742.00110276  -2363.55199832
N      5
  0.8163116315E-01  3.309861012      1.263859789
 -0.289077146585  0.969559096017  0.188564767651
  1420.42046140  179.497004906  -4502.06281827
H      6
  0.3397648290      4.282238175      1.150118576
  1.61148454066  0.226154277628  -1.85353507376
 -211.829050206  8.69615241810  582.485560836
H      7
  0.3206461388      3.055091351      2.214099989
 -2.03187469313  2.87697534416  1.13833147274
 -1114.90916399  -545.986008866  2221.90564473
H      8
  -0.9276867995      3.267504996      1.196961377
 -0.274687593925  2.61813916975  -1.07231596792
 -194.096652901  86.0105795801  1175.08856824
N      9
  0.5906775194      -0.1382972220      1.274500480
  0.626587978760  -1.36573251375  -1.47544707259
 -137.482551177  -3276.79220236  2151.46502944
H     10
  0.3727784551      0.8113735355      0.9993044583
 -0.528970091169  -2.22997037374  -3.54286940300
  159.952718104  2605.70943862  -1157.15571441
H     11
  0.2544671322      -0.7400256748      0.5329631432
  1.75300767940  -3.35785154800  -0.369635322360
  141.573812999  430.989613333  -455.381299014
H     12
  1.600118475      -0.2158729261      1.276274652
  0.729894449241  -0.785005794749E-02  -0.879729398939
  189.924261711  528.249914019  -643.935983080

```

The CONFIG file has the same format as the output file REVCON. When restarting from a previous run of DL_POLY_2, the CONFIG file must be replaced by the REVCON file, which is renamed as the CONFIG file. For each atom, first, second and third rows are the cartesian coordinates, velocities and forces, respectively.

The FIELD file contains the force field information defining the nature of the molecular forces. Our FIELD file is shown below.

Sistema NH3_3

```

units kcal
molecules 1
NH3
nummols 3
atoms 4
N          14.0067  -0.982200
1
H          1.00794  0.327400
3
rigid 1
      4  1  2  3  4
finish
vdw 1
N          N          pav1  0.296500
6.700 6.000 3.931
close

```

Sistema ammoniac líquid

```

units kcal
molecules 1
NH3
nummols 512
atoms 4
N          14.0067  -1.080420
1
H          1.00794  0.360140
3
rigid 1
      4  1  2  3  4
finish
vdw 1
N          N          pav1  0.012856
6.700 6.000 3.931
close

```